

ABSTRACT

4
5 The stratospheric polar vortex is weaker in the easterly phase of the quasi-biennial oscillation (QBO-E) than in the westerly phase (QBO-W), but the mechanism behind the QBO's
6 influence is not well understood. We argue firstly that the composite difference of the atmospheric state between QBO-E and QBO-W closely resembles the structure of the Northern
7 Annular Mode (NAM), the leading empirical orthogonal function of stratospheric variability,
8 including its wave components. Studies of dynamical systems indicate that many different
9 forcings could give rise to this response, and therefore this composite difference does not
10 provide information about the forcing mechanism. The transient response of the vortex to
11 forcing by the QBO is probably much more informative, particularly on time scales shorter
12 than the dynamical time scale of vortex variability, which is about a week. This response
13 in a general circulation model is consistent with the proposed mechanism of Holton and
14 Tan (1980) but does not show the signature of several proposed mechanisms in which the
15 tropical lower stratospheric winds are not important. Our novel approach of examining the
16 transient response to a forcing on short time scales may be useful in various other outstanding
17 problems.
18
19

1. Introduction

The most prominent feature of the wintertime polar stratosphere is the westerly vortex that forms around the pole. The Northern Hemisphere (NH) winter vortex is more variable than its Southern Hemisphere counterpart, with breakdowns of the vortex known as major stratospheric sudden warmings (SSWs) happening about six times per decade on average (Charlton and Polvani 2007). As well as being theoretically interesting, understanding how external factors influence this variability may help improve seasonal forecasts of the NH troposphere as it has become realised that weakenings of the vortex give rise to a more negative tropospheric Northern Annular Mode (NAM) (e.g. Baldwin and Dunkerton 1999, 2001; Jung and Barkmeijer 2006).

Holton and Tan (1980) showed that the vortex is influenced by the quasi-biennial oscillation (QBO) (Baldwin et al. 2001; Gray 2010; Anstey and Shepherd 2013). The QBO is a phenomenon that dominates variability in the equatorial lower stratosphere whereby the zonal mean zonal wind (ZMW) direction on a given pressure level alternates between being easterly and westerly, with the easterly and westerly wind regimes descending with time from the upper to the lower stratosphere. The QBO phase is normally defined as easterly (QBO-E) or westerly (QBO-W) according to the sign of the ZMW in the lower stratosphere. The average period is 28 months. The vortex is weaker on average in the easterly QBO phase than in the westerly phase by over 10 ms^{-1} (Holton and Tan 1980; Pascoe et al. 2005). This “Holton-Tan (HT) relationship” has also been found in atmospheric models of varying complexity (e.g. O’Sullivan and Young 1992; Hamilton 1998; Gray et al. 2003; Calvo et al. 2007).

Understanding the mechanism behind this relationship is important for having confidence in observations of apparent non-linear interactions with other forcings, such as with the solar cycle (e.g. Labitzke 2005; Camp and Tung 2007) and the El Niño-Southern Oscillation (ENSO) (e.g. Garfinkel and Hartmann 2007; Wei et al. 2007) and in the seasonal timing of the effect, which is still not well reproduced by models – the only modelling study to

47 report a statistically significant HT relationship in November, when the correlation between
48 equatorial and vortex ZMW is greatest in observations, is Anstey et al. (2010). It is
49 also important for knowing what models must represent well in order to reproduce the HT
50 relationship and exhibit realistic vortex variability.

51 The explanation for the HT relationship put forward by Holton and Tan (1980) in-
52 volved the equatorial winds influencing the waveguide for extratropical planetary waves.
53 Low-wavenumber stationary planetary waves dominate wave forcing of the extratropical NH
54 stratosphere. The surface in the tropics where the ZMW is zero (also referred to as the
55 “zero wind line”) is a critical surface for these waves. Holton and Tan (1980) referred to
56 the work of Tung (1979) who argued this surface ought to reflect planetary waves back to-
57 wards the pole. In QBO-E, the critical surface in the lower stratosphere is moved polewards
58 into the NH subtropics, so Holton and Tan (1980) suggested this would concentrate wave
59 activity in the NH polar region, weakening the vortex. Henceforth this will be referred to
60 as the “Holton-Tan mechanism”. The work of Tung (1979) was based on linear wave theory
61 for which wave amplitudes are assumed to be small, unlike in the real stratosphere, but
62 later work showed the critical surface ought to be reflecting of eddy zonal momentum flux
63 in the time-averaged sense even if wave amplitudes become large (Killworth and McIntyre
64 1985). Physically this is because if the critical surface sustained absorption of eddy mo-
65 mentum flux then the critical layer would continually widen (Haynes 2003), which cannot
66 happen indefinitely as its width cannot exceed the size of the Earth. (However, the critical
67 layer may be absorbing at certain times as long as this is balanced by over-reflection at
68 other times.) This depends on several assumptions, such as that the fluid motion is two
69 dimensional and that vorticity is conserved in the region being mixed by planetary waves.
70 These assumptions are not strictly met in the real stratosphere, where there is dissipation of
71 wave activity by diabatic and viscous processes and motion is three dimensional; the critical
72 surfaces in the tropics must be at least partially absorbing of eddy zonal momentum flux
73 to be consistent with the observed overall convergence of the flux in the tropics on monthly

74 time scales (Andrews et al. 1987).

75 Composite analysis has been used to test the HT mechanism. In observations the geopo-
76 tential height (GPH) wavenumber-1 amplitude and upward component of the Eliassen-Palm
77 (EP) flux (Andrews et al. 1987), which is commonly used as an indicator of planetary wave
78 propagation, are greater in November and December in QBO-E, but in January and Febru-
79 ary these values are greater during QBO-W (although the difference in these months is
80 not highly statistically significant) (Holton and Tan 1980; Ruzmaikin et al. 2005). Holton
81 and Tan (1982) and Hu and Tung (2002) considered the January–February data not to be
82 consistent with the HT mechanism.

83 Modelling studies using GCMs indicate that on average in winter there is a greater
84 upward component of the EP flux into the high-latitude stratosphere from the troposphere
85 and greater EP flux convergence in the stratosphere during QBO-E than during QBO-W
86 (e.g. Hamilton 1998; Calvo et al. 2007), although the locations of these effects differ between
87 models. Holton and Austin (1991) and O’Sullivan and Dunkerton (1994) found that the
88 amplitude of planetary waves peaks faster in QBO-E in perpetual winter runs in primitive
89 equation models. These results have been interpreted as being broadly consistent with the
90 HT mechanism.

91 Kodera (1991) suggested that the ZMW anomalies associated with the QBO merid-
92 ional circulation (Baldwin et al. 2001) may also affect planetary wave propagation, but this
93 has been given less attention until fairly recently. Ruzmaikin et al. (2005) suggested the
94 meridional circulation may directly affect the vortex by advection of potential temperature.

95 Naoe and Shibata (2010) argued that according to the HT mechanism the mid-latitude
96 lower stratospheric EP flux ought to be more poleward in QBO-E, yet this is not the
97 case. Their analysis of composite differences of EP flux between QBO-E and QBO-W in
98 a chemistry-climate model led them to argue that the QBO meridional circulation has an
99 important role in the HT relationship and that the shift of the critical surface in the lower
100 stratosphere is not important. Garfinkel et al. (2012) reached a similar conclusion by ex-

101 amining the transient response to nudging equatorial winds towards QBO-E in a general
102 circulation model (GCM) without coupled chemistry. Yamashita et al. (2011) also argued
103 that the HT mechanism was not consistent with composite differences of EP flux between
104 QBO-E and QBO-W in their chemistry-climate model, and proposed that the southwards
105 critical surface shift in the upper stratosphere is more important than the northwards shift
106 in the lower stratosphere.

107 However, experiments with a primitive equation model showed that the vortex is more
108 disturbed when equatorial winds are relaxed towards a constant easterly value at all heights,
109 which would not be expected to produce a strong meridional circulation due to the lack of
110 vertical wind shear in the tropics (Gray et al. 2003), or towards easterly jets (Gray et al.
111 2004). These results suggest that neither the meridional circulation nor a southwards shift of
112 the upper stratospheric critical surface are necessary to produce the HT relationship. This
113 raises the questions of whether GCMs behave differently to the primitive equation model
114 or whether the effects of shifts in the critical surface at different heights do not combine
115 linearly.

116 Section 2 of this paper describes the observational data, the GCM and the diagnostics
117 we have used. In section 3 we argue that the composite difference of the atmospheric state
118 between the QBO phases closely resembles the signature of the stratospheric NAM and that
119 this is not likely to be helpful for understanding the mechanism behind the HT relationship,
120 in observations or models. In section 4 we argue the full transient response of the vortex to
121 imposing a QBO-E or QBO-W state at the Equator is likely to be much more informative,
122 especially the response shortly after this forcing is applied. We examine this response in a
123 GCM in section 5 and show the easterly acceleration of the ZMW in the tropical lower
124 stratosphere can directly cause increased EP flux convergence and zonal wind deceleration
125 in the high latitude NH stratosphere, consistent with the HT mechanism. We do not see
126 the responses in the eddy momentum flux predicted by other proposals in which the QBO
127 meridional circulation or the upper stratospheric critical surface plays an important role.

128 We conclude based on these results and on the results of Gray et al. (2003, 2004) that the
129 HT mechanism is the most likely explanation for the HT relationship (section 6).

130 **2. Data and methods**

131 *a. Observational data*

132 We use the ERA-40 reanalysis (Uppala et al. 2005) on standard pressure levels from
133 September 1957 to August 2002 to examine the HT relationship in observations. Randel
134 et al. (2004) found that ERA-40 matches stratospheric measurements of the zonal mean
135 circulation derived from radiosonde, rocketsonde and lidar measurements quite closely and
136 performs quite well compared to other analyses and re-analyses, although errors may be
137 substantial in the upper stratosphere above about 5 hPa. Baldwin and Gray (2005) found
138 the ERA-40 QBO to agree well with independent rocketsonde data. ERA-40 agrees well
139 with other analyses in its representation of SSWs (Charlton and Polvani 2007).

140 For analysis of our ERA-40 data we define the QBO as being in its easterly or west-
141 erly phase when the 5S–5N November–February mean ZMW is easterly or westerly respec-
142 tively at 50hPa, the pressure at which the correlation between the November–February mean
143 ZMW averaged over 5S–5N and that at (60N, 10 hPa) is greatest.

144 *b. Northern Annular Mode index*

145 We compare the QBO-E minus QBO-W EP flux and GPH differences to the EP flux
146 signature of the stratospheric NAM, the leading empirical orthogonal function (EOF) of the
147 extratropical stratosphere. We index the NAM by the leading principal component of the
148 monthly-mean GPH north of 20N between 1–100 hPa, weighted by pressure and the cosine
149 of the latitude, calculated using the method of Baldwin et al. (2009). This is similar to the
150 NAM index of Thompson and Wallace (2000), but restricted to the stratosphere. We also

151 reverse the usual sign convention, so that when the index is positive the vortex is weaker,
152 to more easily compare the NAM signature with the QBO-E minus QBO-W differences.
153 Then at each latitude and pressure, the EP flux components and its divergence are linearly
154 regressed against the index, such that the presented signature corresponds to a one standard
155 deviation increase in our NAM index. This is done separately for each calendar month. The
156 correlation between this index and the leading principal components of GPH on individual
157 pressure levels 10 hPa and 50 hPa is 0.97 or greater in each calendar month November–
158 February and the correlation with that at 5 hPa is 0.75 or above, so this index captures
159 variability throughout the NH stratosphere well.

160 *c. GCM simulations*

161 We have performed experiments using the Met Office HadGEM2-CCS GCM. This coupled
162 ocean-atmosphere model has a well-resolved stratosphere, with 60 atmospheric levels in the
163 vertical up to 84 km altitude (corresponding to a pressure of approximately 0.01 hPa) and
164 atmospheric horizontal resolution 1.25° in latitude and 1.875° in longitude. The model
165 includes parameterised orographic gravity wave drag up to 40 km height, using the scheme of
166 Webster et al. (2003), and non-orographic gravity wave drag (NOGWD), using the scheme
167 of Warner and McIntyre (1999) as implemented by Scaife et al. (2002). The NOGWD
168 causes the model to exhibit a spontaneous QBO. The model does not include a chemistry
169 scheme. For full model details see Martin et al. (2011). Osprey et al. (2013) found that
170 HadGEM2-CCS exhibits a realistic stratospheric climatology and realistic variability.

171 Results from a 240-year pre-industrial control run, which excludes variability due to
172 changing greenhouse gas concentrations, volcanic eruptions and solar variations, were used
173 to confirm that the model reproduces the HT relationship reasonably well (section 5). The
174 correlation between the November–February mean ZMZW averaged over 5S–5N and that at
175 (60N, 10 hPa) is greatest for equatorial winds at 30 hPa, so the sign of the 5S–5N November–
176 February mean ZMZW on this level is used to define the QBO phase for analysis of model

177 data.

178 Section 5 presents results from experiments designed to examine the transient response
179 of the vortex to nudging towards a QBO-E zonal wind pattern in the tropical stratosphere.
180 We performed a “climatological tropical wind” (ClimEq) control run, which was set up iden-
181 tically to the 240-year pre-industrial control run except that the zonal wind in the tropical
182 stratosphere was nudged towards the ERA-Interim monthly mean climatology between Jan-
183 uary 1979 and December 2010 (with the climatology at each model time step calculated by
184 linear interpolation between the middle of each month). ERA-Interim is likely to have a
185 better representation of the stratosphere above 10 hPa than ERA-40 (Simmons et al. 2007;
186 Uppala et al. 2008), so it is used in preference to create target equatorial zonal wind profiles.
187 The nudging had the effect of eliminating the QBO, but the mean and standard deviation of
188 wintertime extratropical winds were not strongly affected. We then performed 120 “QBO-E”
189 branch runs of length one month, taking initial conditions at January 1 and February 1 of
190 60 different years from the ClimEq run (the first two years of this run were not used to
191 allow the model to adjust to the nudging). In these runs the zonal wind in the tropical
192 stratosphere was nudged towards the ERA-Interim climatology plus a typical QBO-E pro-
193 file. The QBO-E profile was taken as the mean 3D zonal wind anomaly of the 30 months
194 in ERA-Interim with the most negative anomalies in the 5S–5N mean ZMW at 30 hPa,
195 multiplied by a factor of 3 in order to raise the signal to noise ratio of the vortex response
196 (figure 1) – the equatorial ZMW anomaly does not become larger than that in observed
197 QBO-E phases in the time scale of 8 days considered in section 5, so this just affects the
198 rate at which equatorial winds adopt a QBO-E profile. This method is similar to that used
199 by Garfinkel et al. (2012), but importantly we focus on the vortex response at shorter times
200 after nudging towards the QBO-E profile is begun.

201 Nudging was carried out between 21.25S and 21.25N and was implemented by subtracting
202 $\alpha(\phi)(u - u^T)$ from the change in the zonal wind calculated at the end of each time step at
203 each gridpoint, where u is the zonal wind, u^T is the target nudging profile and ϕ is the

204 latitude. The nudging parameter $\alpha(\phi)$ is given by

$$\alpha(\phi) = \frac{1}{20 \text{ days}} e^{-2(\phi/16^\circ)^2}$$

205 between heights of 17.4–39.1 km (corresponding to pressure range 3.3–84.3 hPa). At one
206 model level below and above this range (16.3 km, 103 hPa and 40.9 km, 2.6 hPa) α was set
207 to one half its value within the range and is zero at other heights. The nudging code was
208 adapted from that developed as part of the UKCA project (Telford et al. 2008). The vertical
209 profile of the 5S–5N mean ZMW differences between the QBO-E runs and the ClimEq run
210 is very similar to that in figure 1 between about 3–100 hPa over the first 8 days, although
211 the meridional width of the nudged QBO-E winds is only 2/3 that of the target profile due
212 to the weakness of the nudging away from the Equator (not shown) – this would most likely
213 cause the influence on the vortex to be weaker than for a perfect imposed QBO-E profile.

214 *d. Diagnostic tools and statistical methods*

215 We present the influence of the QBO on the EP flux $\mathbf{F} = (F^\phi, F^z)$ (Andrews et al.
216 1987), which is usually taken to show the negative of the zonal mean zonal momentum
217 flux associated with zonal asymmetries. F^ϕ is analagous to the negative of the eddy zonal
218 momentum flux $-\overline{u'v'}$ that was considered by Killworth and McIntyre (1985) in their analysis
219 of the reflectivity of the critical line in their analytical model, where u' and v' are departures
220 from the zonal mean zonal and meridional components of the wind respectively and the
221 overbar indicates zonal averaging. We present the acceleration term $D_F = (\rho_0 a \cos \phi)^{-1} \nabla \cdot \mathbf{F}$
222 to show where the EP flux is convergent or divergent, where $\rho_0(z)$ is a reference density profile
223 and a is the Earth’s radius.

224 Statistical significances of the QBO-E minus QBO-W composite differences in the EP
225 flux components and in the GPH were calculated according to a Monte Carlo permutation
226 test. Each year was assigned to a surrogate QBO-E or QBO-W group at random, and the
227 composite difference between these random groups was calculated. This was repeated 1,000

228 times to find the probability distribution of the differences at each grid-point under the null
229 hypothesis that there is no dependence of these variables on the QBO, and the probability
230 that the magnitude of the difference would exceed that of the difference in the data.

231 To test the statistical significance of the mean differences between the model branch runs
232 nudged to QBO-E and the ClimEq run, a Monte Carlo bootstrap technique was used (Efron
233 and Tibshirani 1993). At each gridpoint a surrogate data sample was generated according to
234 the null hypothesis that the mean difference is zero but other moments of the true distribution
235 of differences equal those in the data. The mean of the differences for all pairs of branch and
236 control runs was subtracted from the difference for each pair and the results were resampled
237 with replacement. The probability of the mean of this resampled data being larger than
238 that for the real data was estimated using 1,000 data resamplings. All significance tests are
239 two-tailed.

240 **3. The observed influence of the QBO on the wave part** 241 **of the stratospheric circulation**

242 Figure 2 shows the QBO-E minus QBO-W composite difference in the monthly mean
243 NH EP flux and D_F from November to February in ERA-40. In agreement with the findings
244 of previous studies (e.g Dunkerton and Baldwin 1991; Ruzmaikin et al. 2005), the EP flux
245 is more upward in November and December north of 55N, but this signal is not present in
246 January and February, and it has been argued that the late-winter signal is not consistent
247 with the HT mechanism (Holton and Tan 1982). In all months there is a poleward EP
248 flux difference in the tropical lower stratosphere, indicating the equatorward flux is less in
249 QBO-E. This is restricted to latitudes south of about 25N, and Naoe and Shibata (2010)
250 and Yamashita et al. (2011) argued that this means reflection of eddy zonal momentum flux
251 from the lower stratospheric easterlies in QBO-E cannot be directly influencing the vortex.
252 There is greater EP flux convergence in the high-latitude stratosphere in November, and a

253 region of greater convergence that moves downwards from the middle to lower stratosphere
254 between December and February.

255 Figure 3 shows the regression of the EP flux against our NAM index, showing the anomaly
256 associated with a weaker vortex (note our choice of sign of the index as explained in sec-
257 tion 2b). There is a striking resemblance to the QBO-E minus QBO-W composite differ-
258 ences in each calendar month in the extratropics. The flux is more upward north of 55N in
259 November and December and near 45N and 80N in January and more downward near 60N
260 in January and February.

261 There is a similar correspondence between the QBO-E minus QBO-W composite differ-
262 ence and the NAM signature of GPH. Figure 4 shows the QBO-E minus QBO-W composite
263 difference in the monthly mean NH 10 hPa GPH from November to February in ERA-40.
264 The climatological eddy component, defined as the climatological GPH with the zonal mean
265 subtracted, is also shown. Figure 5 shows the signature of the NAM in NH 10 hPa GPH,
266 which bears a very good resemblance to the GPH differences between QBO-E and QBO-W.
267 Anomaly correlations with the NAM signature north of 20N, calculated with gridpoints
268 weighted by the square root of the cosine of the latitude, are indicated below the compos-
269 ite GPH differences in figure 4. The correlations are between 0.75 and 0.95 in November–
270 January, with a lower correlation in February when the differences are not highly statistically
271 significant. The correlations are all greater if only anomalies north of 60N are considered,
272 so this is not simply arising from a direct influence of the QBO on the subtropics.

273 In November, the top left panel of figure 4 shows GPH is greater in QBO-E over the
274 Canadian Arctic and less over northern Europe. This represents positive interference with the
275 wavenumber-1 part of the climatological wave pattern, and so the wavenumber-1 amplitude
276 is greater, whilst the wavenumber-2 amplitude is slightly less (figure 6). Over the course
277 of winter, however, the pattern shifts so that more positive GPH is found over the Arctic
278 and north Atlantic with lower GPH over the North Pacific in January and February. This
279 gives weak destructive interference with the climatological waves, so wavenumber-1 and 2

280 amplitudes are both slightly reduced. Figure 6 also shows the change in the wavenumber-1
281 and 2 amplitudes at 60N if the NAM signature in GPH multiplied by the QBO-E minus
282 QBO-W composite difference in the index is added to the climatological GPH, showing that
283 the observed changes in the wave amplitudes in QBO-E versus QBO-W correspond closely
284 to the seasonal evolution of the NAM signature.

285 Previous work has noted that the QBO-E minus QBO-W composite difference of ZMW
286 is very similar to the NAM signature (Dunkerton and Baldwin 1991; Kodera 1995; Ruzmaikin
287 et al. 2005), but here we show that this is true for the EP flux and GPH wave amplitude
288 differences as well, which is important given that these differences have been used to try to
289 understand the mechanism of the QBO's influence.

290 A correspondence between the leading EOF of a system and its response to an applied
291 forcing is a commonly observed feature of dynamical systems, if the response is averaged over
292 time scales that are long compared to the dynamical time scales. Palmer and Weisheimer
293 (2011) illustrate that in the simple system of Lorenz (1963) (that which gives rise to the
294 famous Lorenz butterfly attractor), applying a steady force in any direction in the xy -
295 plane gives rise to a shift in the system's mean state which is very nearly aligned with
296 the system's leading EOF, so the spatial pattern of the response closely resembles that of
297 the leading EOF. Ring and Plumb (2008) found in a tropospheric GCM that the steady-
298 state response to various mechanical and thermal forcings applied in the extratropics closely
299 resembles the tropospheric NAM. Branstator and Selten (2009) examine the reasons why the
300 response to greenhouse gas forcing in a tropospheric GCM is NAM-like. They conclude that
301 it largely results from a linear effect whereby anomalies in the NAM tend to persist for a
302 long time, so the NAM is a prominent pattern in natural variability and in the response to a
303 forcing after time-averaging. This behaviour is also predicted by the fluctuation-dissipation
304 theorem (Gritsun and Dymnikov 1999), which has been argued to apply approximately to
305 the atmosphere (e.g. Leith 1975; Gritsun and Branstator 2007).

306 Invoking this behaviour, which seems robust in atmospheric models and also present

307 in simpler systems like that of Lorenz (1963), can then explain the seasonal evolution of
308 the pattern of EP flux differences in QBO-E and QBO-W, and supports the suggestion of
309 Dunkerton and Baldwin (1991) that the QBO “excited a fundamental...mode of variability
310 in the extratropical atmosphere”. We do not know of any studies that have examined this
311 phenomenon in the stratosphere. It does however seem consistent with previous literature
312 identifying the stratospheric NAM as a prominent pattern that appears not just in response
313 to the QBO but also to other important natural influences on the vortex (volcanic eruptions
314 (e.g. Kodera 1995; Stenchikov et al. 2006), ENSO (e.g. Sassi et al. 2004) and the solar cycle
315 (e.g. Kodera 1995; Labitzke 2005)).

316 Importantly, this behaviour implies that examining the response to a forcing averaged
317 over a long time or using compositing does not in general yield information about the forc-
318 ing mechanism. Observing an anomaly in response to an unknown forcing that resembles
319 the leading EOF does not allow the nature of the forcing to be deduced if many different
320 forcings can give rise to this response. Therefore, the HT mechanism is consistent with the
321 vortex response to the QBO as it simply predicts there should be enough anomalous EP flux
322 convergence in the high-latitude stratosphere in QBO-E to cause deceleration of the vortex,
323 as is observed, and the above discussion indicates this may manifest itself as a modulation
324 of the NAM in composite analysis. However, these observations could also be consistent
325 with other mechanisms that predict a weakening of the vortex during QBO-E. Furthermore,
326 structure in the extratropical QBO-E minus QBO-W composite differences seems to be pri-
327 marily related to the NAM signature rather than the forcing mechanism, and is not a reliable
328 indicator of the mechanism.

329 Another way to understand the difficulty in using these composite differences to infer the
330 forcing mechanism behind the HT relationship is that the differences in the wave components
331 of the flow have contributions not only from the QBO-E equatorial wind pattern but also
332 the effect of the weaker vortex, as changes in the zonally symmetric component of the flow
333 will cause changes in the wave components. What is required is a way of computing the

334 changes due to QBO-E whilst the vortex state is close to constant.

335 4. Motivating examination of the short-term transient 336 response

337 Here we argue that whilst the QBO-E minus QBO-W composite difference cannot be
338 relied on to show the mechanism of the QBO's influence, the full time-dependent transient
339 response should be much more useful.

340 If the forcing mechanism is simple (meaning it does not influence the system in question
341 in a series of intermediate steps), then the response on short time scales following application
342 of the forcing can be expected to show the mechanism clearly. Consider a system described
343 by state vector $\mathbf{x}(t)$ that evolves according to equations

$$\dot{\mathbf{x}}(t) = \mathcal{L}(\mathbf{x}(t), t), \quad (1)$$

344 where the equations may be non-linear and are explicitly time-dependent for generality.
345 The equations governing atmospheric motion may be expressed in this form. Consider also
346 a forced variant of this system described by state vector $\mathbf{x}'(t)$ which evolves according to
347 similar equations with the addition of a state- and time-dependent forcing term,

$$\dot{\mathbf{x}}'(t) = \mathcal{L}(\mathbf{x}'(t), t) + \mathbf{f}(\mathbf{x}'(t), t) \quad (2)$$

348 with $\mathbf{x}(0) = \mathbf{x}'(0) = \mathbf{x}_0$. In the context of the HT relationship, \mathbf{x}' would represent the vortex
349 state and \mathbf{f} the influence of the QBO. Then as long as the difference between the state vectors
350 $\delta\mathbf{x} = \mathbf{x}'(t) - \mathbf{x}(t)$ is analytic, which will be the case if both $\mathbf{x}(t)$ and $\mathbf{x}'(t)$ are analytic, $\delta\mathbf{x}(t)$
351 can be evaluated for small t by writing its Taylor series (in index notation using summation
352 convention) to give

$$\delta x_a(t) = f_a(\mathbf{x}_0, 0)t + \left(\frac{\partial \mathcal{L}_a}{\partial x_b} \Big|_{(\mathbf{x}, t)=(\mathbf{x}_0, 0)} \delta x_b(0) + \frac{df_a}{dt} \Big|_{(\mathbf{x}, t)=(\mathbf{x}_0, 0)} \right) \frac{t^2}{2} + \mathcal{O}(t^3). \quad (3)$$

353 Thus for short times, the difference between the systems is nearly proportional to the applied
 354 forcing at $t = 0$, when this is non-zero. State-dependence of the equations of motion (non-
 355 zero $\partial\mathcal{L}_a/\partial x_b$) acts to complicate the relationship between $\delta\mathbf{x}$ and the forcing as t increases
 356 and may be expected to become important on a time scale of the order of the system’s
 357 dynamical time scale. (If $\mathbf{f}(\mathbf{x}_0, 0) = 0$, it can similarly be shown that $\delta\mathbf{x}(t)$ is proportional
 358 to $d\mathbf{f}/dt|_{(\mathbf{x}, t)=(\mathbf{x}_0, 0)}$ to $\mathcal{O}(t^2)$ when this is non-zero, which is relevant for the results of the
 359 nudging experiments in section 5.) Examining the system’s response on short time scales
 360 shows the effect of the forcing before effects due to the change in the state of the system
 361 become large.

362 If the forcing mechanism unfolds in several steps then the short-term transient response
 363 would be expected to show the steps that develop up to a time scale of the order of the
 364 dynamical time scale, which may still give useful information for testing hypotheses.

365 For studies of the atmosphere, it is probably necessary to use a numerical model to eval-
 366 uate the transient response. Using observations would require identifying two near-identical
 367 atmospheric states with different values of the forcing in question, which is practically im-
 368 possible.

369 **5. The transient response of the vortex to QBO-E forc-** 370 **ing**

371 Firstly we show the HT relationship in the HadGEM2-CCS GCM. Figure 7 shows
 372 the QBO-E minus QBO-W composite difference in the January–February mean ZMW
 373 in ERA-40 and in the 240-year pre-industrial control run of HadGEM2-CCS – the monthly-
 374 mean difference is not statistically significant earlier in winter in HadGEM2-CCS. The model
 375 reproduces the weakening of the vortex seen in observations, with ZMW differences that are
 376 somewhat smaller at high latitudes. The lack of a HT relationship in November and Decem-
 377 ber in the model may be due to the equatorial winds simply having too weak an influence on

378 the vortex, and it taking time for their impact to accumulate and give rise to an appreciable
379 vortex response, following the suggestion of O’Sullivan and Young (1992). It could also be
380 related to the model exhibiting slightly less total variability than in observations in early
381 winter (Osprey et al. 2013), which is a common problem in stratosphere-resolving GCMs. As
382 noted in section 1, few modelling studies have reported an HT relationship in early winter.
383 The mechanism by which the equatorial winds influence the vortex in the model is likely to
384 be qualitatively similar to the mechanism in the real atmosphere.

385 Figure 8 shows the QBO-E minus QBO-W composite difference in the monthly mean NH
386 EP flux in January and February in the model. In these months the model reproduces the
387 pattern of the observed influence of the QBO on the EP flux well, with greater upward flux in
388 the high-latitude stratosphere in January in QBO-E and more poleward and downward flux in
389 February, bearing in mind that the observed differences are not highly statistically significant.
390 The EP flux differences are somewhat smaller than in ERA-40, however, consistent with the
391 ZMWZ differences being smaller.

392 We have examined the transient response of the vortex to nudging equatorial winds
393 towards a QBO-E state on a time scale of about a week, which is comparable to the mid-
394 stratosphere’s dynamical time scale. Figure 9 shows the mean over our ensemble of QBO-E
395 branch runs of the difference in the ZMWZ between the branch runs and the ClimEq run.
396 The QBO-E pattern of winds is visible in the tropics, with mid-latitude anomalies that arise
397 due to the Coriolis force acting on the QBO meridional circulation. The extratropical winds
398 in the lower stratosphere initially strengthen and this appears to be associated with the cells
399 of the QBO meridional circulation. However, between days 5–8 following the start of the
400 nudging there is a weakening of the upper stratospheric winds which descends with time, as
401 expected from the HT relationship.

402 Figure 10 shows the mean difference in the EP flux between the branch runs and the
403 ClimEq run. On days 1–2 between ~ 15 – 30 N the EP flux is more equatorward in the lower
404 stratosphere and poleward in the middle and upper stratosphere. Between days 3–8, how-

405 ever, EP flux differences become statistically significant at higher latitudes. The EP flux is
406 more poleward in the lower stratosphere and more equatorward in the upper stratosphere,
407 extending to the polar region by days 5–6. This is associated with increased EP flux con-
408 vergence in the high-latitude stratosphere between ~ 2 –20 hPa, which is consistent with the
409 weakening of the winds in this region in figure 9. The initial increased absorption of EP
410 flux in the lower stratosphere in days 1–2 next to the critical surface followed by increased
411 reflection seems consistent with the “Stewartson–Warn–Warn” solution for the critical layer
412 discussed by Killworth and McIntyre (1985).

413 The more poleward EP flux from the tropics to the high latitudes is the signal that Naoe
414 and Shibata (2010) argued should be present if the HT mechanism is correct. Our results
415 are thus consistent with the HT mechanism and indicate that increased reflection of eddy
416 zonal momentum flux in QBO-E may directly affect the polar stratosphere. Thus the HT
417 mechanism cannot be ruled out of playing a part in the HT relationship as argued in recent
418 studies. Note that this signal is unlike the QBO-E minus QBO-W composite differences in
419 the EP flux in any calendar month (figure 2), illustrating the necessity of examining the
420 transient response to understand the influence of the QBO.

421 However, it is not just the tropical lower stratospheric easterly wind acceleration that
422 matters – the westerly acceleration above 10 hPa appears to cause a more equatorward
423 EP flux that decreases its convergence at high latitudes, reducing the QBO influence there.
424 Figure 11 shows the EP flux differences using the “acceleration scaling” defined by Gray et al.
425 (2003), to indicate the size of the acceleration associated with the flux. By days 7–8 there is
426 more poleward flux in the QBO-E runs at 1 hPa and above which appears associated with
427 the tropical ZMW at these heights becoming more easterly (figure 9). Easterly anomalies
428 at these altitudes are also observed in QBO-E in winter (Pascoe et al. 2005). Although
429 the magnitude of this momentum flux is small, it is associated with EP flux convergence
430 and deceleration of the ZMW in the mid-latitude upper stratosphere. If the vortex state
431 is sensitive to ZMW changes in this region then this provides a way for tropical upper

432 stratospheric wind changes to contribute to the HTR, as suggested by Gray et al. (2001a,b).

433 These results do not indicate that the EP flux convergence in the high-latitude strato-
434 sphere arises due to other recently proposed mechanisms discussed in section 1 – the EP
435 flux differences have the opposite sign to those predicted by Naoe and Shibata (2010) and
436 Yamashita et al. (2011) and its convergence in mid-latitudes has opposite sign to that pre-
437 dicted by Garfinkel et al. (2012). It is not clear if there are reasons why the signatures of
438 these mechanisms would take more than 8 days to appear, but these results make it seem
439 less likely that any of these mechanisms are dominant.

440 The greater reflection of EP flux in the lower stratosphere in the QBO-E runs occurs
441 despite the zero wind line (ZWL) shifting both poleward and equatorward on different levels
442 below 10 hPa. As remarked in section 2c, the QBO profile is too narrow meridionally, and
443 the ZWL shift may have been more pronounced if this were not the case. The $ZMZW=c$
444 lines show a poleward shift on average at all levels between 15–80 hPa by up to a few degrees
445 for $-5 \text{ m/s} \leq c \leq -2 \text{ m/s}$. The greater reflection in the QBO-E runs may therefore be
446 associated with waves with small negative phase velocities. As the critical surfaces are
447 partially absorbing (section 1), it may also be due to EP flux associated with stationary
448 waves being affected by the ZMWZ south of the ZWL. It is not clear that the ZWL should
449 be considered fundamental given it is unclear whether wave phase velocities can be defined
450 in the subtropics, and the EP flux may be affected by tropical ZMWZ in a region of finite
451 width.

452 The QBO meridional circulation has roughly the same strength relative to the equatorial
453 ZMWZ differences in our branch runs as in the free-running model, indicating that if this
454 circulation were having a substantial direct effect on the vortex then it should be evident
455 in our results. The maximum 10S–10N mean difference in the downwelling of the resid-
456 ual meridional circulation (Andrews et al. 1987) between the branch runs and the ClimEq
457 run over days 7–8 after branching, which is at 15 hPa, is $1.8 \times 10^{-4} \text{ m/s}$. The QBO-E mi-
458 nus QBO-W difference in this quantity divided by two in the pre-industrial control run is

459 1.3×10^{-4} m/s. The ratio of these quantities is 1.4. The ratio of the peak equatorial wind
460 differences in the lower stratosphere between the branch runs and the ClimEq run averaged
461 over days 7–8 (-20 m/s) and the QBO-E minus QBO-W composite peak equatorial wind
462 differences in the pre-industrial control run divided by two (-11 m/s) is 1.8. These ratios
463 are quite similar, indicating that the meridional circulation has about the correct strength
464 in our experiment.

465 The ensemble-mean results we present show the average effect of nudging towards a
466 QBO-E state but may hide sensitivity to the initial conditions. The theory of critical layers
467 only indicates they may be absorbing for finite time periods and the influence of the QBO
468 may be different in such periods. The QBO influence may also be reduced if critical surfaces
469 exist in mid-latitudes. Gray et al. (2003) suggest the QBO may have a weaker influence if
470 the tropospheric wave forcing is very strong or very weak as well.

471 The signal loses statistical significance after day 8, which appears to be because the
472 standard deviation of the differences between the runs grows exponentially with time (not
473 shown), as expected from exponential perturbation growth in a chaotic system such as the
474 atmosphere. The ZMW and EP flux differences between the branch and ClimEq runs grow
475 approximately linearly with time over the first week, and so the loss of statistical significance
476 is consistent with this signal continuing to grow but the noise growing more quickly so that
477 the signal to noise ratio decreases with time. The magnitude of the noise must saturate
478 after some time at the level of the climatological variability. The fact that there is an HT
479 relationship in the 240-year pre-industrial control run implies that the signal to noise ratio
480 would be large enough again after several months for the signal to be statistically significant,
481 implying that the signal would continue to increase in time. Seeing the full evolution of the
482 vortex response to QBO-E forcing in this model would likely require a prohibitive amount of
483 computing resources, and similar experiments with computationally cheaper models may be
484 helpful to understand the transient response fully. The transient response to nudging towards
485 QBO-E presented by Garfinkel et al. (2012) appears to be more statistically significant, but

486 the model they used has unrealistically low vortex variability, which may be part of the
487 reason for the difference.

488 It should be considered whether the use of nudging in the tropical stratosphere would
489 cause differences between the coupling between the tropics and extratropics in our model
490 runs and in the real stratosphere. Previous studies have used nudging of equatorial winds
491 to examine the HT relationship and have obtained realistic results (e.g. Hamilton 1998;
492 Garfinkel et al. 2012), implying that the nudging does not drastically interfere with the
493 coupling between the tropics and extratropics. The nudging we have used would tend to
494 dampen wave activity in the tropical region with time scales longer than a couple of weeks.
495 The most unrealistic effect of the nudging may be to create a QBO profile that is too narrow
496 meridionally, which may weaken the extratropical response. We see no reason why these
497 effects would qualitatively change the interaction between the tropics and extratropics.

498 The atmospheric response to an applied forcing at short times following application of the
499 forcing is indicative of the whole forcing mechanism only if the steps of the mechanism unfold
500 on a time scale less than about the system’s dynamical time scale, so mechanisms whose
501 early stages are consistent with our results but which also involve subsequent steps cannot be
502 ruled out. Our results also do not rule out the meridional circulation having a role through
503 modifying the background state through which the eddy zonal momentum propagates. Our
504 experiments also show the effect of nudging towards QBO-E from a state having close to
505 climatological equatorial winds – as the winds approach a full-strength QBO-E state, the
506 vortex response may depend non-linearly on further increases in the strength of the QBO-E
507 profile. This could be explored in a similar way to our method, using a control run nudged
508 towards a QBO-E state with branch runs nudged towards a stronger QBO-E state. In our
509 runs the equatorial ZMW differences do reach the approximate magnitude of the anomalies
510 in the QBO-E phase in observations in the time scale considered here, however, allowing the
511 possibility that non-linearity will show an effect, so we do not expect that the effects of
512 non-linearity with respect to the equatorial winds would greatly change our results. Our

513 results leave open the question of whether the HT mechanism can account quantitatively for
514 the HT relationship.

515 The key innovative part of this work has been to examine the stratospheric response to
516 QBO forcing on time scales that are shorter than or of the order of the mid-stratosphere's
517 dynamical time scale of ~ 1 week, so we see the response to QBO-E forcing alone before the
518 circulation has evolved. If our EP flux differences are averaged over the first 16 days, as
519 done by Garfinkel et al. (2012), then the poleward EP flux difference from the tropics to
520 high latitudes is no longer apparent.

521 **6. Summary and conclusions**

522 We have discussed investigations into the mechanism by which the QBO influences the
523 stratospheric polar vortex. Understanding this mechanism is important for improving sea-
524 sonal forecasts of the vortex, and therefore also of the troposphere (e.g. Baldwin and Dunker-
525 ton 2001), for understanding non-linear interactions of this relationship with other forcings
526 such as the solar cycle (e.g. Labitzke 2005) and ENSO (e.g. Garfinkel and Hartmann 2007)
527 and understanding the seasonal timing of the effect. Previous observational and modelling
528 studies, when considered together, have not come down firmly in favour of any of the pro-
529 posed mechanisms.

530 We have shown that composite differences of the wave components of the stratospheric
531 circulation between QBO-E and QBO-W are very similar to the signature of the NAM, the
532 leading EOF in the stratosphere. This behaviour is qualitatively similar to that of other
533 dynamical systems, in that different forcings applied to the same system are found to give a
534 response similar to that system's leading EOF. We have argued that this implies that QBO-E
535 minus QBO-W composite differences are not likely to be informative about the mechanism
536 behind the HT relationship, since many different mechanisms could give rise to the NAM-like
537 vortex response.

538 We then showed that the full transient response of a system to a given forcing should be
539 much more informative about the forcing mechanism. The system’s transient response on
540 short time scales after application of the forcing will show the steps of the forcing mechanism
541 that unfold up to about one dynamical time scale, about one week in the mid-stratosphere,
542 and will closely resemble the forcing if the forcing mechanism essentially involves only one
543 step.

544 Our examination of the first few days of the transient response of the vortex to nudging
545 of equatorial stratospheric winds towards a QBO-E state in the HadGEM2-CCS GCM in-
546 dicates that the EP flux becomes less equatorwards between the tropics and high latitudes
547 in the lower stratosphere, there is greater convergence of the EP flux in the high-latitude
548 stratosphere between about 2–20 hPa and that the westerly wind in this region decelerates.
549 This is consistent with the hypothesis that more easterly winds in the tropical lower strato-
550 sphere cause greater reflection of eddy zonal momentum flux towards the polar stratosphere,
551 causing deceleration of the westerly winds, as suggested by Holton and Tan (1980). Our re-
552 sults do not show the signatures of the mechanisms suggested by Naoe and Shibata (2010),
553 Yamashita et al. (2011) or Garfinkel et al. (2012) who proposed that the role of the lower
554 stratospheric zero wind line is less important than that of the QBO meridional circulation
555 or the upper stratospheric zero wind line. Combining this with the results of Gray et al.
556 (2003, 2004), which indicate that the meridional circulation and the shift of the zero wind
557 line in the upper stratosphere (in the opposite sense to that in the lower stratosphere) are
558 not essential to produce the HT relationship, we conclude that the mechanism of Holton and
559 Tan (1980) is the most likely explanation for the HT relationship, and that the behaviour
560 of HadGEM2-CCS is consistent with the behaviour of the primitive equation model used
561 by Gray et al. (2003, 2004) in showing that easterly acceleration of tropical winds leads to
562 deceleration of the ZMZW at high latitudes. However, it is not clear if the role of the zero
563 wind line is fundamental and the total anomalous poleward EP flux depends on ZMZW
564 changes throughout the depth of the tropical stratosphere. We have not ruled out a role for

565 the meridional circulation through modifying the background state through which the eddy
566 zonal momentum flux propagates, or mechanisms that include multiple steps that unfold on
567 a time scale greater than about a week.

568 To our knowledge, using the transient response of the atmosphere to a forcing on time
569 scales of a few days to understand the forcing mechanism is novel and may be of use in
570 various other outstanding problems, such as for understanding the downward influence of
571 the stratosphere on the troposphere (e.g. Baldwin and Dunkerton 2001) or the dynamical
572 influence of the solar cycle (e.g Labitzke 2005).

573 *Acknowledgments.*

574 We would like to thank D. Andrews, J. Anstey, S. Osprey and D. Mitchell for helpful
575 discussions and comments, and also P. Telford and M. Dalvi for assistance with implementing
576 nudging in HadGEM2-CCS. P. Watson is supported by a Natural Environment Research
577 Council studentship.

REFERENCES

- 580 Andrews, D., J. Holton, and C. Leovy, 1987: *Middle Atmosphere Dynamics*. Academic Press.
- 581 Anstey, J. and T. Shepherd, 2013: High-latitude influence of the quasi-biennial oscillation.
582 *Q. J. R. Meteorol. Soc.*, in press.
- 583 Anstey, J., T. Shepherd, and J. Scinocca, 2010: Influence of the quasi-biennial oscillation on
584 the extratropical winter stratosphere in an atmospheric general circulation model and in
585 reanalysis data. *J. Atmos. Sci.*, **67** (5), 1402–1419.
- 586 Baldwin, M. and T. Dunkerton, 1999: Propagation of the Arctic oscillation from the strato-
587 sphere to the troposphere. *J. Geophys. Res.*, **104**, 30 937–30 946.
- 588 Baldwin, M. and T. Dunkerton, 2001: Stratospheric harbingers of anomalous weather
589 regimes. *Science*, **294**, 581–584.
- 590 Baldwin, M. and L. Gray, 2005: Tropical stratospheric zonal winds in ECMWF ERA-40
591 reanalysis, rocketsonde data, and rawinsonde data. *Geophys. Res. Lett.*, **32** (9), L09806,
592 doi:10.1029/2004GL022328.
- 593 Baldwin, M., D. Stephenson, and I. Joliffe, 2009: Spatial weighting and iterative projection
594 methods for EOFs. *J. Climate*, **22** (2), 234–243.
- 595 Baldwin, M., et al., 2001: The quasi-biennial oscillation. *Rev. Geophys.*, **39** (2), 179–229.
- 596 Branstator, G. and F. Selten, 2009: “Modes of variability” and climate change. *J. Climate*,
597 **22** (10), 2639–2658.
- 598 Calvo, N., M. Giorgetta, and C. Peña Ortiz, 2007: Sensitivity of the boreal winter circulation
599 in the middle atmosphere to the quasi-biennial oscillation in MAECHAM5 simulations. *J.*
600 *Geophys. Res.*, **112**, D10124, doi:10.1029/2006JD007844.

- 601 Camp, C. and K. Tung, 2007: The influence of the solar cycle and QBO on the late-winter
602 stratospheric polar vortex. *J. Atmos. Sci.*, **64** (4), 1267–1283.
- 603 Charlton, A. and L. Polvani, 2007: A new look at stratospheric sudden warmings. Part I:
604 Climatology and modeling benchmarks. *J. Climate*, **20**, 449–469.
- 605 Dunkerton, T. and M. Baldwin, 1991: Quasi-biennial modulation of planetary-wave fluxes
606 in the Northern Hemisphere winter. *J. Atmos. Sci.*, **48** (8), 1043–1061.
- 607 Efron, B. and R. J. Tibshirani, 1993: *An introduction to the bootstrap*. Chapman and Hall,
608 New York.
- 609 Garfinkel, C. and D. Hartmann, 2007: The effects of the quasi-biennial oscillation and the
610 El Nino Southern Oscillation on polar temperatures in the stratosphere. *J. Geophys. Res.*,
611 **112**, D19112, doi:10.1029/2007JD008481.
- 612 Garfinkel, C. I., T. A. Shaw, D. L. Hartmann, and D. W. Waugh, 2012: Does the Holton-Tan
613 mechanism explain how the quasi-biennial oscillation modulates the Arctic polar vortex?
614 *J. Atmos. Sci.*, **69** (5), 1713–1733.
- 615 Gray, L., 2010: Equatorial Dynamics. *The Stratosphere: Dynamics, Transport and Chem-*
616 *istry, Geophys. Monogr. Series*.
- 617 Gray, L., S. Crooks, C. Pascoe, S. Sparrow, and M. Palmer, 2004: Solar and QBO influences
618 on the timing of stratospheric sudden warmings. *J. Atmos. Sci.*, **61** (23), 2777–2796.
- 619 Gray, L., E. Drysdale, B. Lawrence, and T. Dunkerton, 2001a: Model studies of the inter-
620 annual variability of the northern-hemisphere stratospheric winter circulation: The role of
621 the quasi-biennial oscillation. *Q. J. R. Meteorol. Soc.*, **127** (574), 1413–1432.
- 622 Gray, L., S. Phipps, T. Dunkerton, M. Baldwin, E. Drysdale, and M. Allen, 2001b: A
623 data study of the influence of the equatorial upper stratosphere on northern-hemisphere
624 stratospheric sudden warmings. *Q. J. R. Meteorol. Soc.*, **127** (576), 1985–2003.

- 625 Gray, L., S. Sparrow, M. Jukes, A. O'Neill, and D. Andrews, 2003: Flow regimes in the
626 winter stratosphere of the Northern Hemisphere. *Q. J. R. Meteorol. Soc.*, **129** (589),
627 925–945.
- 628 Gritsun, A. and G. Branstator, 2007: Climate response using a three-dimensional operator
629 based on the fluctuation-dissipation theorem. *J. Atmos. Sci.*, **64** (7), 2558–2575.
- 630 Gritsun, A. and V. Dymnikov, 1999: Barotropic atmosphere response to small external
631 actions: Theory and numerical experiments. *Izvestiya, Atmospheric and Oceanic Physics*,
632 **35** (5), 511–525.
- 633 Hamilton, K., 1998: Effects of an imposed quasi-biennial oscillation in a comprehensive
634 troposphere-stratosphere-mesosphere general circulation model. *J. Atmos. Sci.*, **55** (14),
635 2393–2418.
- 636 Haynes, P., 2003: Critical layers. *Encyclopedia of Atmospheric Sciences*, **2**, 582–589.
- 637 Holton, J. and J. Austin, 1991: The influence of the equatorial QBO on sudden stratospheric
638 warmings. *J. Atmos. Sci.*, **48** (4), 607–618.
- 639 Holton, J. and H. Tan, 1980: The influence of the equatorial quasi-biennial oscillation on
640 the global circulation at 50 mb. *J. Atmos. Sci.*, **37** (10), 2200–2208.
- 641 Holton, J. and H. Tan, 1982: The quasi-biennial oscillation in the Northern Hemisphere
642 lower stratosphere. *J. Meteor. Soc. Japan*, **60**, 140–148.
- 643 Hu, Y. and K. Tung, 2002: Tropospheric and equatorial influences on planetary-wave am-
644 plitude in the stratosphere. *Geophys. Res. Lett.*, **29** (2), doi:10.1029/2001GL013762.
- 645 Jung, T. and J. Barkmeijer, 2006: Sensitivity of the tropospheric circulation to changes in the
646 strength of the stratospheric polar vortex. *Monthly Weather Review*, **134** (8), 2191–2207.
- 647 Killworth, P. and M. McIntyre, 1985: Do Rossby-wave critical layers absorb, reflect, or
648 over-reflect? *Journal of Fluid Mechanics*, **161**, 449–492.

649 Kodera, K., 1991: The solar and equatorial qbo influences on the stratospheric circulation
650 during the early Northern-Hemisphere winter. *Geophys. Res. Lett.*, **18 (6)**, 1023–1026,
651 doi:10.1029/90GL02298.

652 Kodera, K., 1995: On the origin and nature of the interannual variability of the winter
653 stratospheric circulation in the Northern-hemisphere. *J. Geophys. Res.*, **100 (D7)**, 14 077–
654 14 087.

655 Labitzke, K., 2005: On the solar cycle-QBO relationship: a summary. *Journal of Atmo-*
656 *spheric and Solar-Terrestrial Physics*, **67 (1-2)**, 45–54.

657 Leith, C., 1975: Climate response and fluctuation dissipation. *J. Atmos. Sci.*, **32 (10)**,
658 2022–2026.

659 Lorenz, E., 1963: Deterministic nonperiodic flow. *J. Atmos. Sci.*, **20 (2)**, 130–141.

660 Martin, G., et al., 2011: The HadGEM2 family of Met Office Unified Model Climate config-
661 urations. *Geoscientific Model Development Discussions*, **4**, 765–841.

662 Naoe, H. and K. Shibata, 2010: Equatorial quasi-biennial oscillation influence on north-
663 ern winter extratropical circulation. *J. Geophys. Res.*, **115**, D19102, doi:10.1029/
664 2009JD012952.

665 Osprey, S., L. Gray, S. Hardiman, N. Butchart, and T. Hinton, 2013: Stratospheric variability
666 in 20th Century CMIP5 simulations of the Met Office climate model: High-top versus low-
667 top. *J. Climate*, **26 (5)**, 1607–1625.

668 O’Sullivan, D. and T. Dunkerton, 1994: Seasonal development of the extratropical QBO in
669 a numerical model of the middle atmosphere. *J. Atmos. Sci.*, **51 (24)**, 3706–3706.

670 O’Sullivan, D. and R. Young, 1992: Modeling the quasi-biennial oscillation’s effect on the
671 winter stratospheric circulation. *J. Atmos. Sci.*, **49 (24)**, 2437–2448.

672 Palmer, T. N. and A. Weisheimer, 2011: Diagnosing the causes of bias in climate models -
673 why is it so hard? *Geophysical and Astrophysical Fluid Dynamics*, **105** (2-3), 351–365.

674 Pascoe, C., L. Gray, S. Crooks, M. Juckes, and M. Baldwin, 2005: The quasi-biennial
675 oscillation: Analysis using ERA-40 data. *J. Geophys. Res.*, **110**, D08105, doi:10.1029/
676 2004JD004941.

677 Randel, W., et al., 2004: The SPARC intercomparison of middle-atmosphere climatologies.
678 *J. Climate*, **17**, 986–1003.

679 Ring, M. J. and R. A. Plumb, 2008: The response of a simplified GCM to axisymmetric
680 forcings: Applicability of the fluctuation-dissipation theorem. *J. Atmos. Sci.*, **65** (12),
681 3880–3898.

682 Ruzmaikin, A., J. Feynman, X. Jiang, and Y. Yung, 2005: Extratropical signature of the
683 quasi-biennial oscillation. *J. Geophys. Res.*, **110**, D11111, doi:10.1029/2004JD005382.

684 Sassi, F., D. Kinnison, B. Boville, R. Garcia, and R. Roble, 2004: Effect of El Nino–Southern
685 Oscillation on the dynamical, thermal, and chemical structure of the middle atmosphere.
686 *J. Geophys. Res.*, **109** (D17), D17108, doi:10.1029/2003JD004434.

687 Scaife, A., N. Butchart, C. Warner, and R. Swinbank, 2002: Impact of a spectral gravity
688 wave parameterization on the stratosphere in the Met Office Unified Model. *J. Atmos.*
689 *Sci.*, **59** (9), 1473–1489.

690 Simmons, A., S. Uppala, D. Dee, and S. Kobayashi, 2007: ERA-Interim: New ECMWF
691 reanalysis products from 1989 onwards. *ECMWF Newsletter*, **110**, 25–35.

692 Stenchikov, G., K. Hamilton, R. Stouffer, A. Robock, V. Ramaswamy, B. Santer, and
693 H. Graf, 2006: Arctic Oscillation response to volcanic eruptions in the IPCC AR4 cli-
694 mate models. *J. Geophys. Res.*, **111**, D07107, doi:10.1029/2005JD006286.

- 695 Telford, P. J., P. Braesicke, O. Morgenstern, and J. A. Pyle, 2008: Technical Note: De-
696 scription and assessment of a nudged version of the new dynamics Unified Model. *Atmos.*
697 *Chem. Phys.*, **8 (6)**, 1701–1712.
- 698 Thompson, D. and J. Wallace, 2000: Annular modes in the extratropical circulation. Part I:
699 Month-to-month variability. *J. Climate*, **13 (5)**, 1000–1016.
- 700 Tung, K., 1979: A theory of stationary long waves. Part III: Quasi-normal modes in a
701 singular waveguide. *Monthly Weather Review*, **107 (6)**, 751–774.
- 702 Uppala, S., D. Dee, S. Kobayashi, P. Berrisford, and A. Simmons, 2008: Towards a climate
703 data assimilation system: status update of ERA-Interim. *ECMWF Newsletter*, **115**, 12–18.
- 704 Uppala, S., et al., 2005: The ERA-40 re-analysis. *Q. J. R. Meteorol. Soc.*, **131 (612)**,
705 2961–3012.
- 706 Warner, C. and M. McIntyre, 1999: Toward an ultra-simple spectral gravity wave parame-
707 terization for general circulation models. *Earth Planets and Space*, **51 (7–8)**, 475–484.
- 708 Webster, S., A. Brown, D. Cameron, and C. Jones, 2003: Improvements to the representation
709 of orography in the Met Office Unified Model. *Q. J. R. Meteorol. Soc.*, **129 (591, Part**
710 **b)**, 1989–2010.
- 711 Wei, K., W. Chen, and R. Huang, 2007: Association of tropical Pacific sea surface temper-
712 atures with the stratospheric Holton-Tan oscillation in the Northern Hemisphere winter.
713 *Geophys. Res. Lett.*, **34**, L16814, doi:10.1029/2007GL030478.
- 714 Yamashita, Y., H. Akiyoshi, and M. Takahashi, 2011: Dynamical response in the northern
715 hemisphere midlatitude and high-latitude winter to the QBO simulated by CCSR/NIES
716 CCM. *J. Geophys. Res.*, **116**, D06118, doi:10.1029/2010JD015016.

717 List of Figures

- 718 1 Left: the zonal mean of the target “QBO-E times 3” zonal wind profile used
719 in the GCM experiments with nudged equatorial winds. Right: the 5S–5N
720 mean of this profile. 34
- 721 2 QBO-E minus QBO-W composite differences in ERA-40 of the wintertime
722 EP flux (arrows, black where either the F^ϕ or F^z differences are statistically
723 significant above the 95% level and grey otherwise) and D_F (contours, plotted
724 at 0.5 m/s/day intervals, with negative contours dotted and a thickened zero
725 contour). The EP flux is shown at pressures 2, 5, 10, 20, 30, 50 and 70 hPa and
726 every 3.75° in latitude. A reference arrow is shown in the top left plot along
727 with its (F^ϕ , F^z) values. Shading shows where D_F differences are statistically
728 significant above the 95% level. 35
- 729 3 Regression of the EP flux and D_F onto our NAM index in ERA-40, showing
730 the anomaly associated with a weaker vortex with our choice of sign of the
731 index, plotted as for the QBO-E minus QBO-W composite differences in fig-
732 ure 2. There is a good correspondence between these regression patterns and
733 the composite differences. 36
- 734 4 QBO-E minus QBO-W composite differences in ERA-40 of the wintertime
735 GPH at 10 hPa (greyscale) north of 20N. White contours show the clima-
736 tological zonally asymmetric component of GPH with contour values ± 200
737 and ± 600 m with negative contours dashed. NAM correlation values indicate
738 the anomaly correlation of the composite differences with the NAM signature
739 north of 20N shown in figure 5. Stippling shows where GPH differences are
740 statistically significant above the 95% level. 37

741 5 Regression of 10 hPa GPH north of 20N onto our NAM index in ERA-40,
742 showing a close resemblance to the QBO-E minus QBO-W composite differ-
743 ences in figure 4. White contours show the climatological zonally asymmetric
744 component of GPH with contour values ± 200 and ± 600 m with negative con-
745 tours dashed. 38

746 6 Lines with filled symbols show the QBO-E minus QBO-W composite differ-
747 ences of GPH wavenumber-1 amplitude (solid lines and circles) and wavenumber-
748 2 amplitude (dotted lines and triangles) at 60N and 10 hPa for months November-
749 February. Lines with unfilled symbols show the differences resulting from
750 adding the NAM signature in GPH multiplied by the QBO-E minus QBO-W
751 composite difference in the NAM index to the climatological GPH, showing
752 that the main qualitative features of the QBO-E minus QBO-W differences in
753 GPH wave amplitudes are largely explained just by QBO modulation of the
754 NAM. 39

755 7 QBO-E minus QBO-W composite differences of January-February mean ZMW
756 in ERA-40 (a) and in HadGEM2-CCS (b). HadGEM2-CCS reproduces the
757 differences in ERA-40 reasonably well, with smaller high-latitude differences.
758 Contour levels are every 4 m/s with negative contours dashed and the zero
759 contour thickened. 40

760 8 As in figure 2 but for HadGEM2-CCS, showing only January and February
761 when the differences are statistically significant. In these months HadGEM2-
762 CCS reproduces the pattern of QBO-E minus QBO-W composite EP flux
763 differences in ERA-40 quite well. 41

- 764 9 Ensemble mean ZMW differences between branch runs nudged towards the
765 QBO-E equatorial wind profile and the ClimEq run averaged over each two
766 day interval up to 8 days following branching. Contours are at 0, ± 0.02 ,
767 ± 0.2 , ± 2 and ± 10 m/s with negative contours dotted and the zero contour
768 thickened. Shading shows where differences are statistically significant at the
769 95% level. 42
- 770 10 Ensemble mean differences between branch runs nudged towards the QBO-E
771 equatorial wind profile and the ClimEq run averaged over each two day interval
772 up to 8 days following branching in EP flux (arrows, shown only where either
773 the F^ϕ or F^z differences are statistically significant above the 95% level) and
774 D_F (contours, at 0, ± 0.02 and ± 0.1 m/s/day, with negative contours dotted
775 and the zero contour thickened). The thick dashed line shows the zero wind
776 line in the days 1–8 mean ZMW in the ClimEq run. The EP flux differences
777 are shown at pressures 0.5, 1, 2, 5, 10, 20, 40 and 100 hPa and every 3.75°
778 in latitude. A reference arrow is shown in the top left of each plot along
779 with its (F^ϕ , F^z) values. Shading shows where D_F differences are statistically
780 significant at the 95% level. 43
- 781 11 As in figure 10 but using “acceleration scaling” of the EP flux vectors as
782 defined by Gray et al. (2003), which indicates the zonal acceleration associated
783 with the flux. A reference arrow is shown in the top left of each plot along
784 with the (F^ϕ , F^z) values it would have at the Equator at 10 hPa. 44

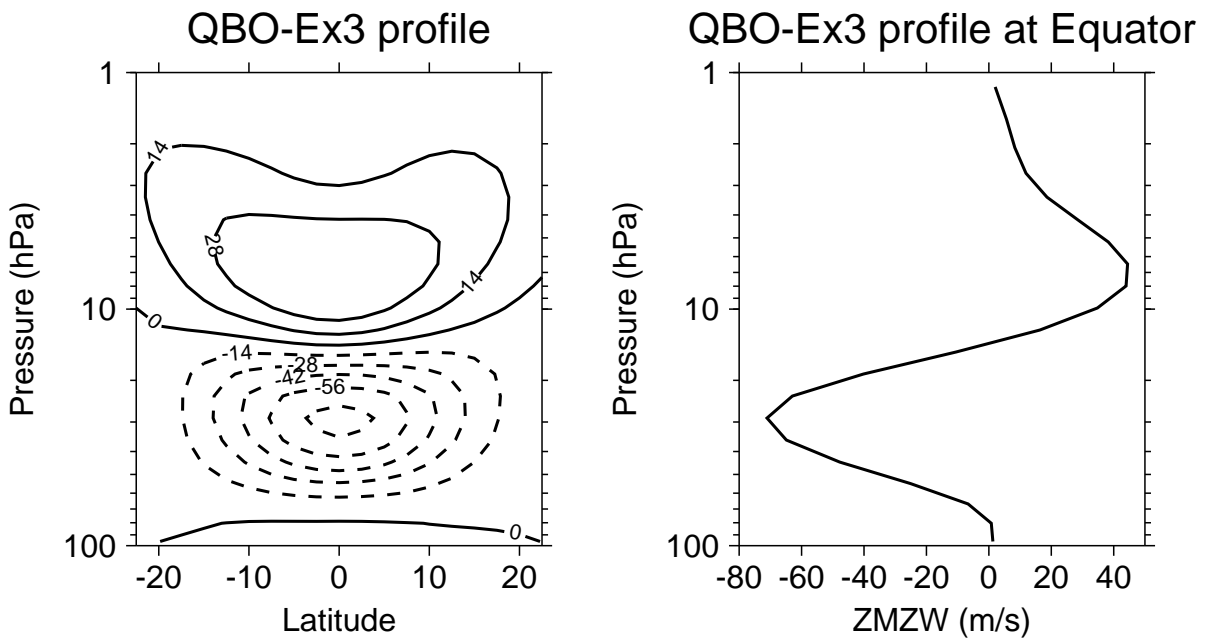


FIG. 1. Left: the zonal mean of the target “QBO-E times 3” zonal wind profile used in the GCM experiments with nudged equatorial winds. Right: the 5S–5N mean of this profile.

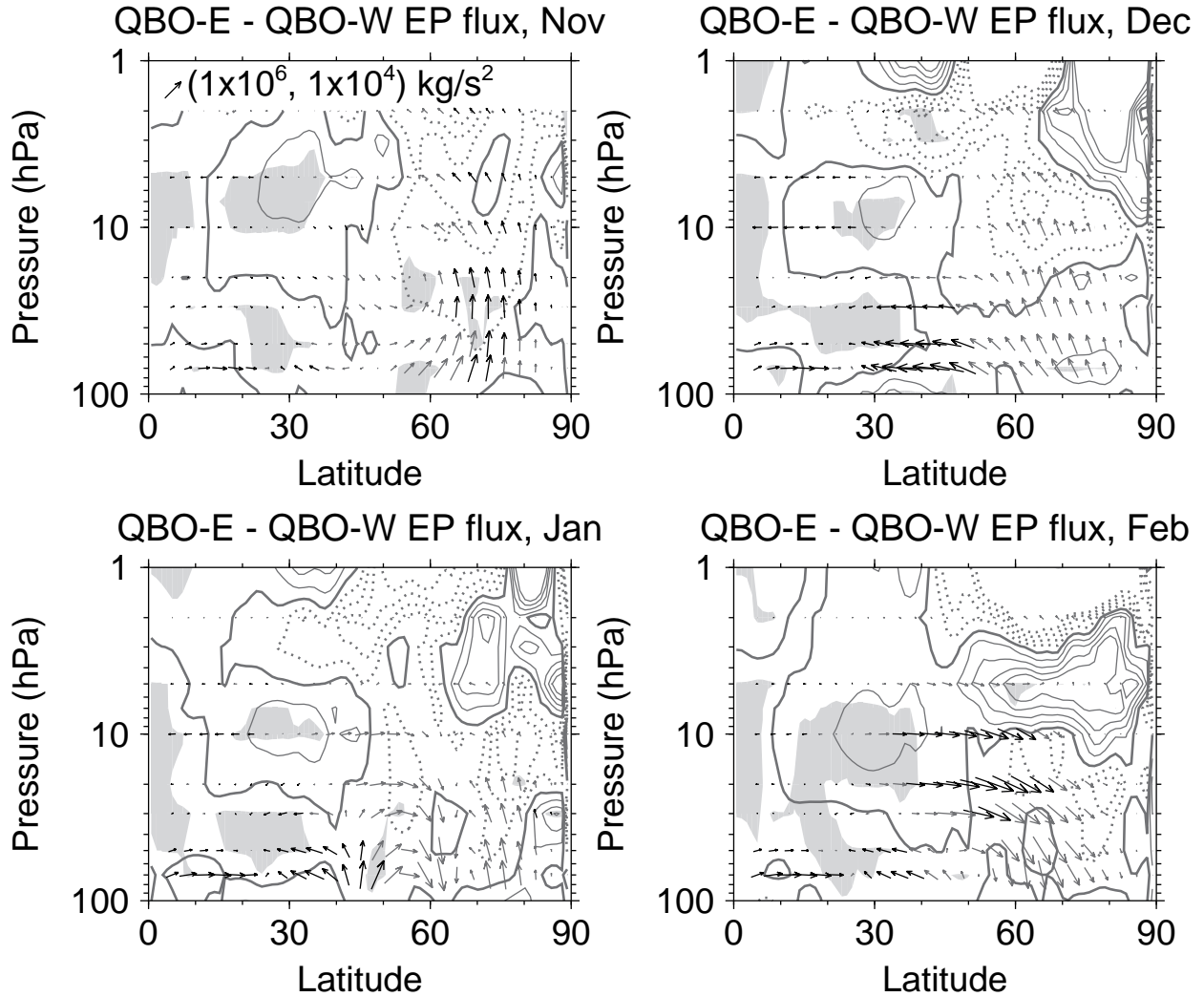


FIG. 2. QBO-E minus QBO-W composite differences in ERA-40 of the wintertime EP flux (arrows, black where either the F^ϕ or F^z differences are statistically significant above the 95% level and grey otherwise) and D_F (contours, plotted at 0.5 m/s/day intervals, with negative contours dotted and a thickened zero contour). The EP flux is shown at pressures 2, 5, 10, 20, 30, 50 and 70 hPa and every 3.75° in latitude. A reference arrow is shown in the top left plot along with its (F^ϕ, F^z) values. Shading shows where D_F differences are statistically significant above the 95% level.

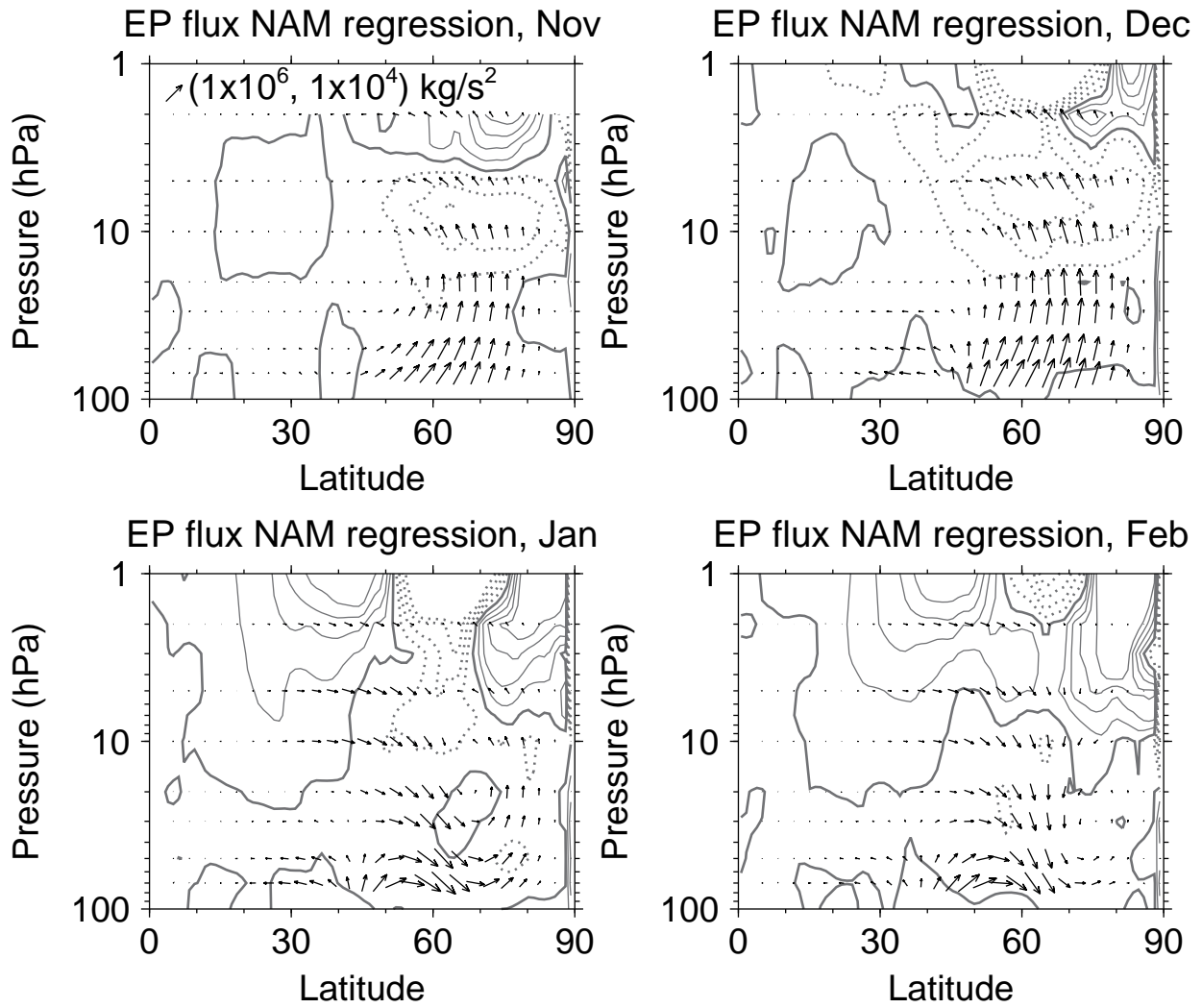


FIG. 3. Regression of the EP flux and D_F onto our NAM index in ERA-40, showing the anomaly associated with a weaker vortex with our choice of sign of the index, plotted as for the QBO-E minus QBO-W composite differences in figure 2. There is a good correspondence between these regression patterns and the composite differences.

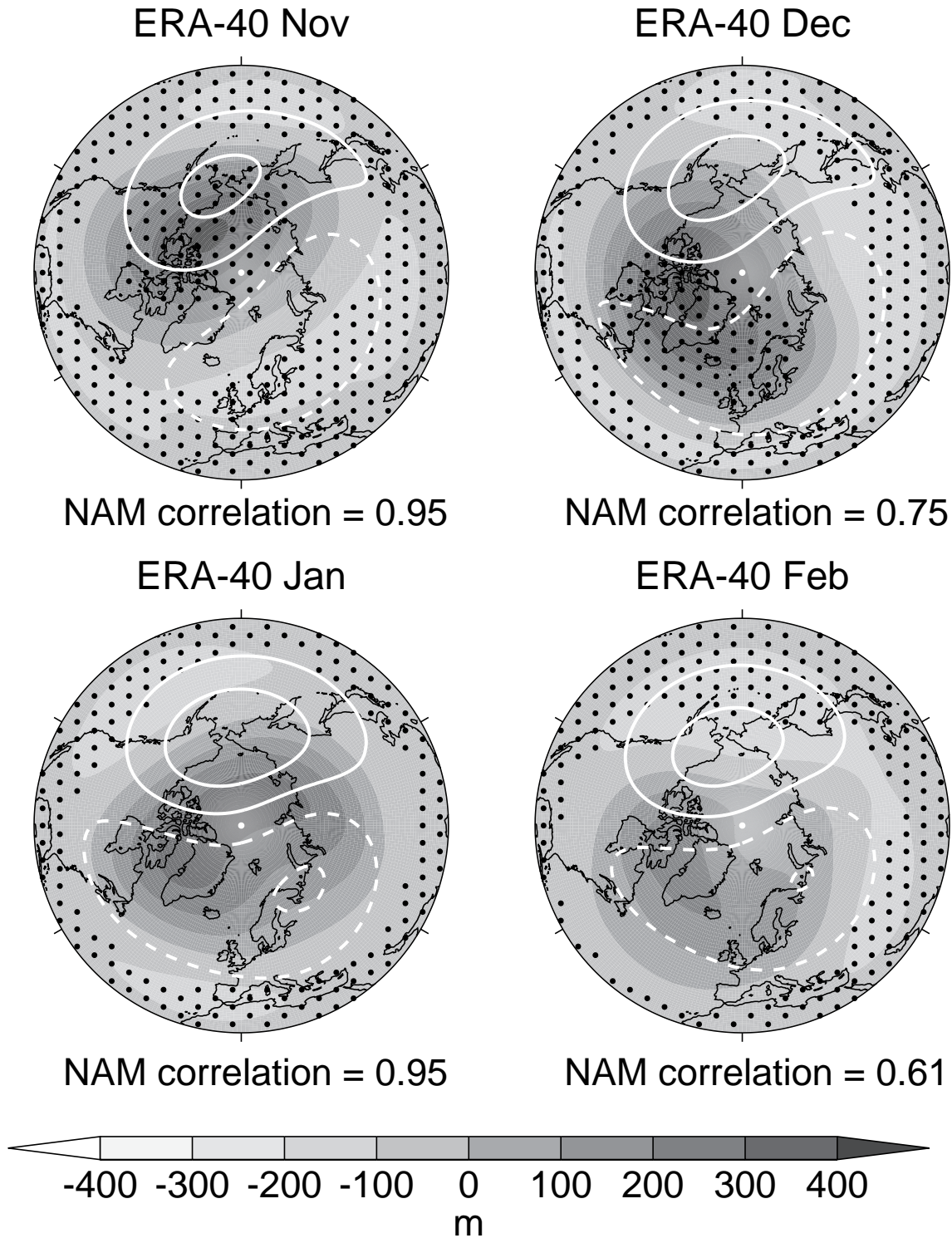


FIG. 4. QBO-E minus QBO-W composite differences in ERA-40 of the wintertime GPH at 10 hPa (greyscale) north of 20N. White contours show the climatological zonally asymmetric component of GPH with contour values ± 200 and ± 600 m with negative contours dashed. NAM correlation values indicate the anomaly correlation of the composite differences with the NAM signature north of 20N shown in figure 5. Stippling shows where GPH differences are statistically significant above the 95% level.

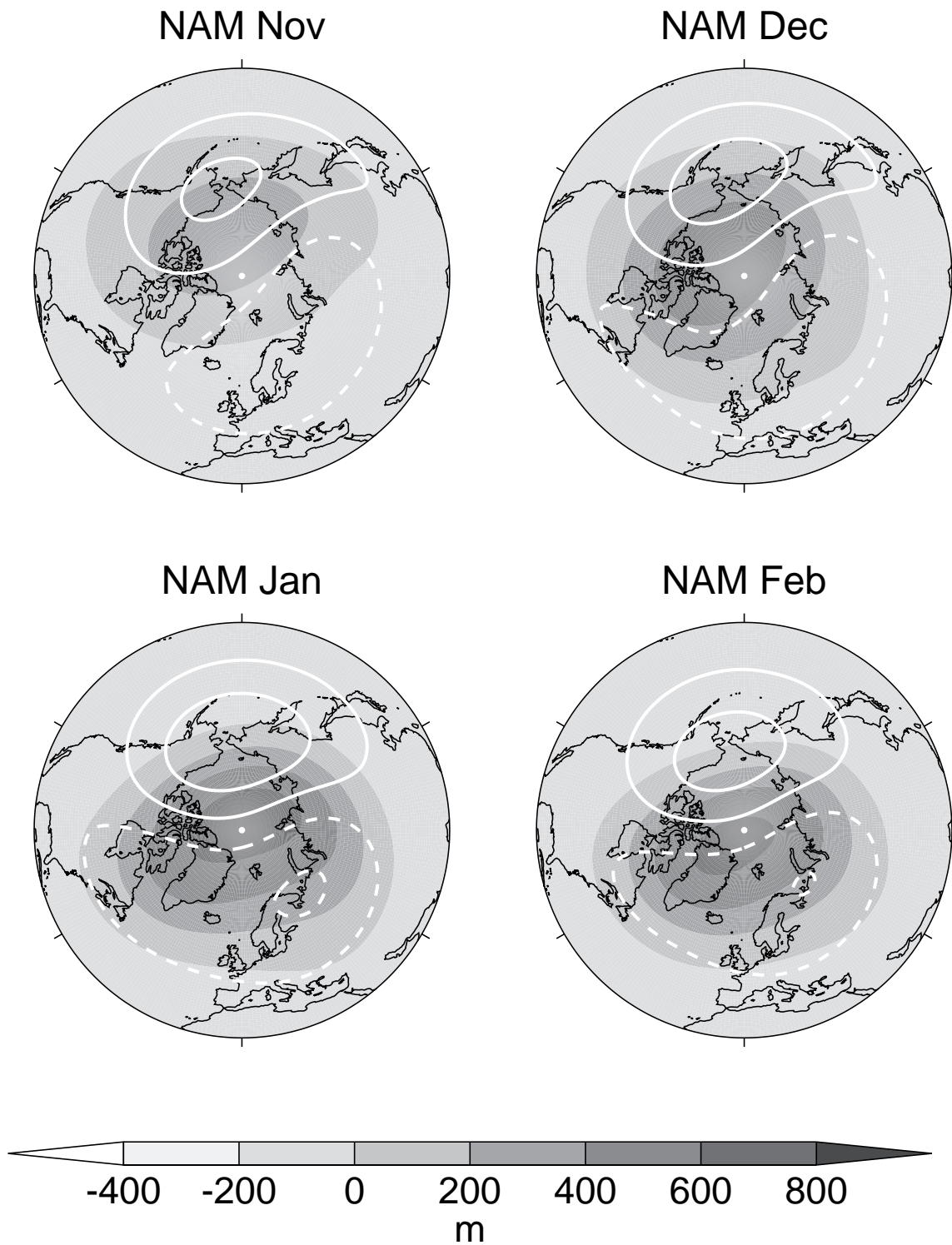


FIG. 5. Regression of 10 hPa GPH north of 20N onto our NAM index in ERA-40, showing a close resemblance to the QBO-E minus QBO-W composite differences in figure 4. White contours show the climatological zonally asymmetric component of GPH with contour values ± 200 and ± 600 m with negative contours dashed.

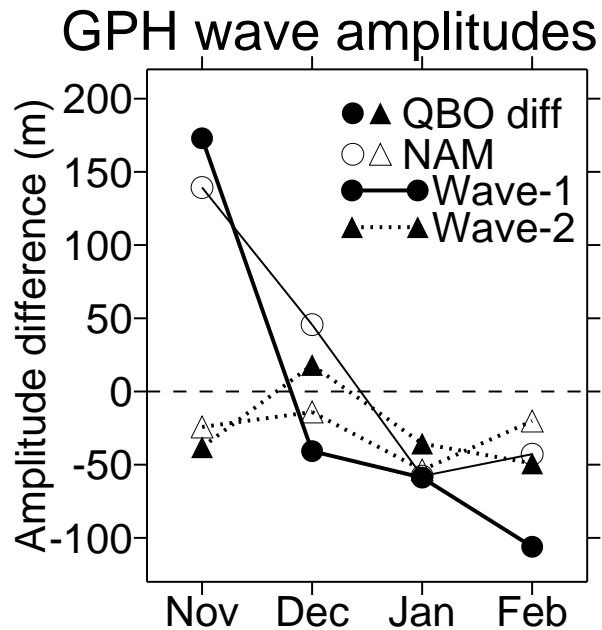


FIG. 6. Lines with filled symbols show the QBO-E minus QBO-W composite differences of GPH wavenumber-1 amplitude (solid lines and circles) and wavenumber-2 amplitude (dotted lines and triangles) at 60N and 10 hPa for months November–February. Lines with unfilled symbols show the differences resulting from adding the NAM signature in GPH multiplied by the QBO-E minus QBO-W composite difference in the NAM index to the climatological GPH, showing that the main qualitative features of the QBO-E minus QBO-W differences in GPH wave amplitudes are largely explained just by QBO modulation of the NAM.

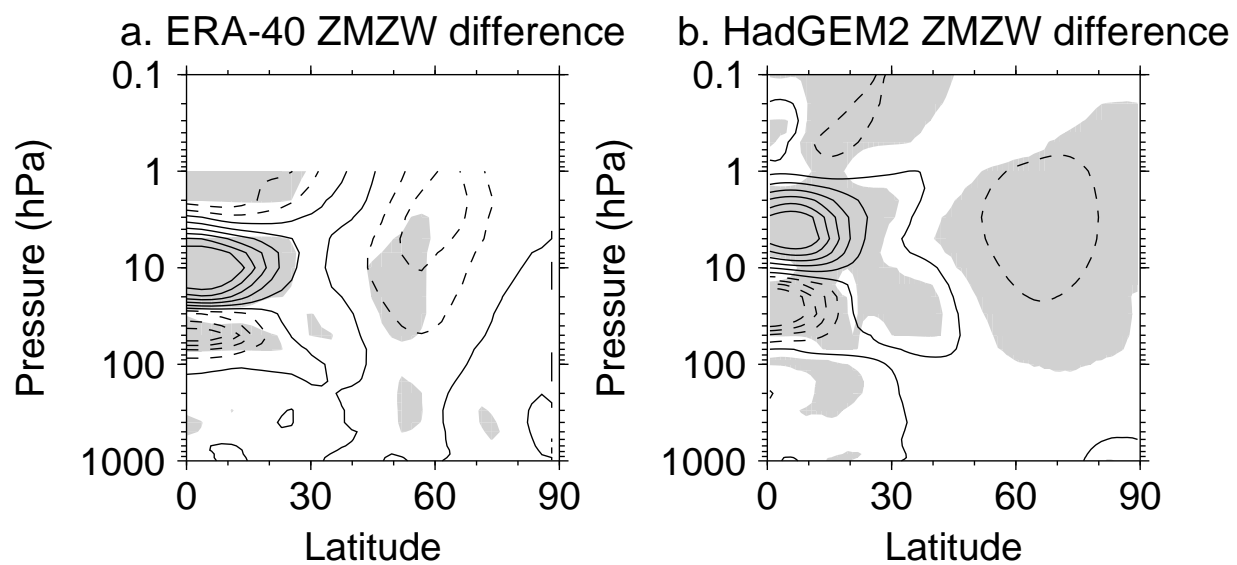


FIG. 7. QBO-E minus QBO-W composite differences of January–February mean ZMW in ERA-40 (a) and in HadGEM2-CCS (b). HadGEM2-CCS reproduces the differences in ERA-40 reasonably well, with smaller high-latitude differences. Contour levels are every 4 m/s with negative contours dashed and the zero contour thickened.

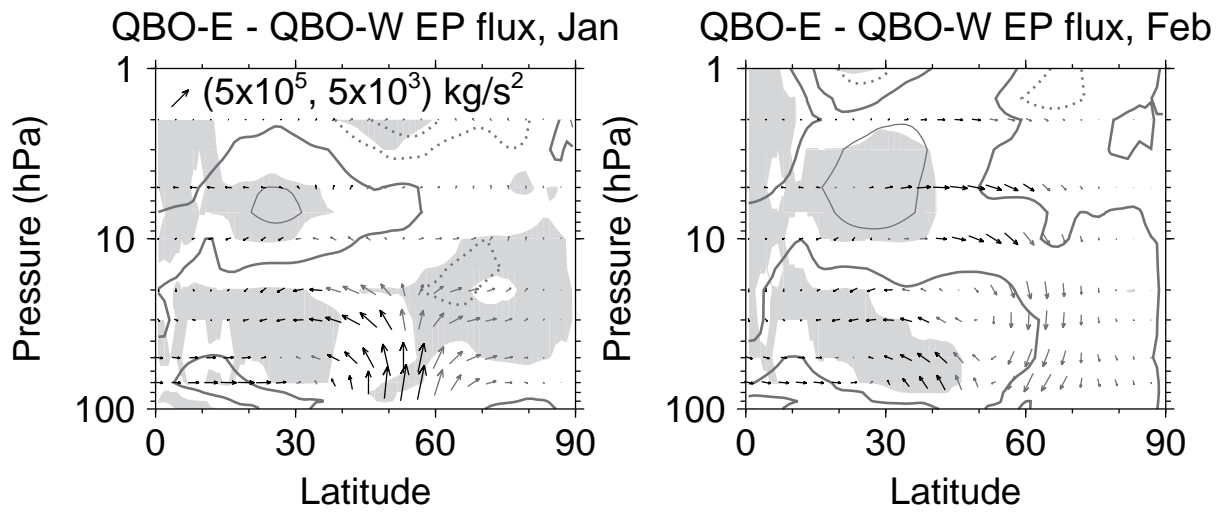


FIG. 8. As in figure 2 but for HadGEM2-CCS, showing only January and February when the differences are statistically significant. In these months HadGEM2-CCS reproduces the pattern of QBO-E minus QBO-W composite EP flux differences in ERA-40 quite well.

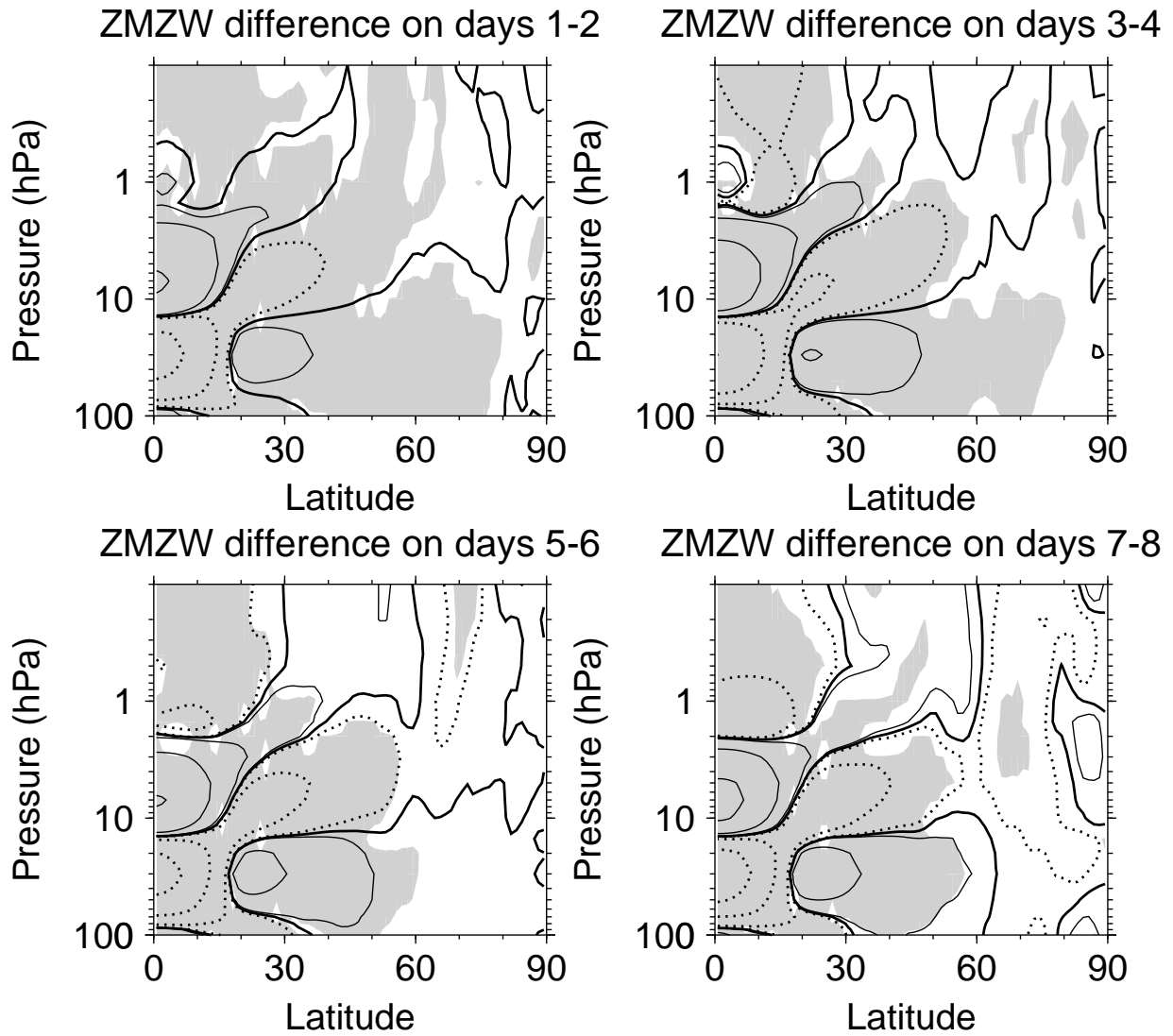


FIG. 9. Ensemble mean ZMW differences between branch runs nudged towards the QBO-E equatorial wind profile and the ClimEq run averaged over each two day interval up to 8 days following branching. Contours are at 0, ± 0.02 , ± 0.2 , ± 2 and ± 10 m/s with negative contours dotted and the zero contour thickened. Shading shows where differences are statistically significant at the 95% level.

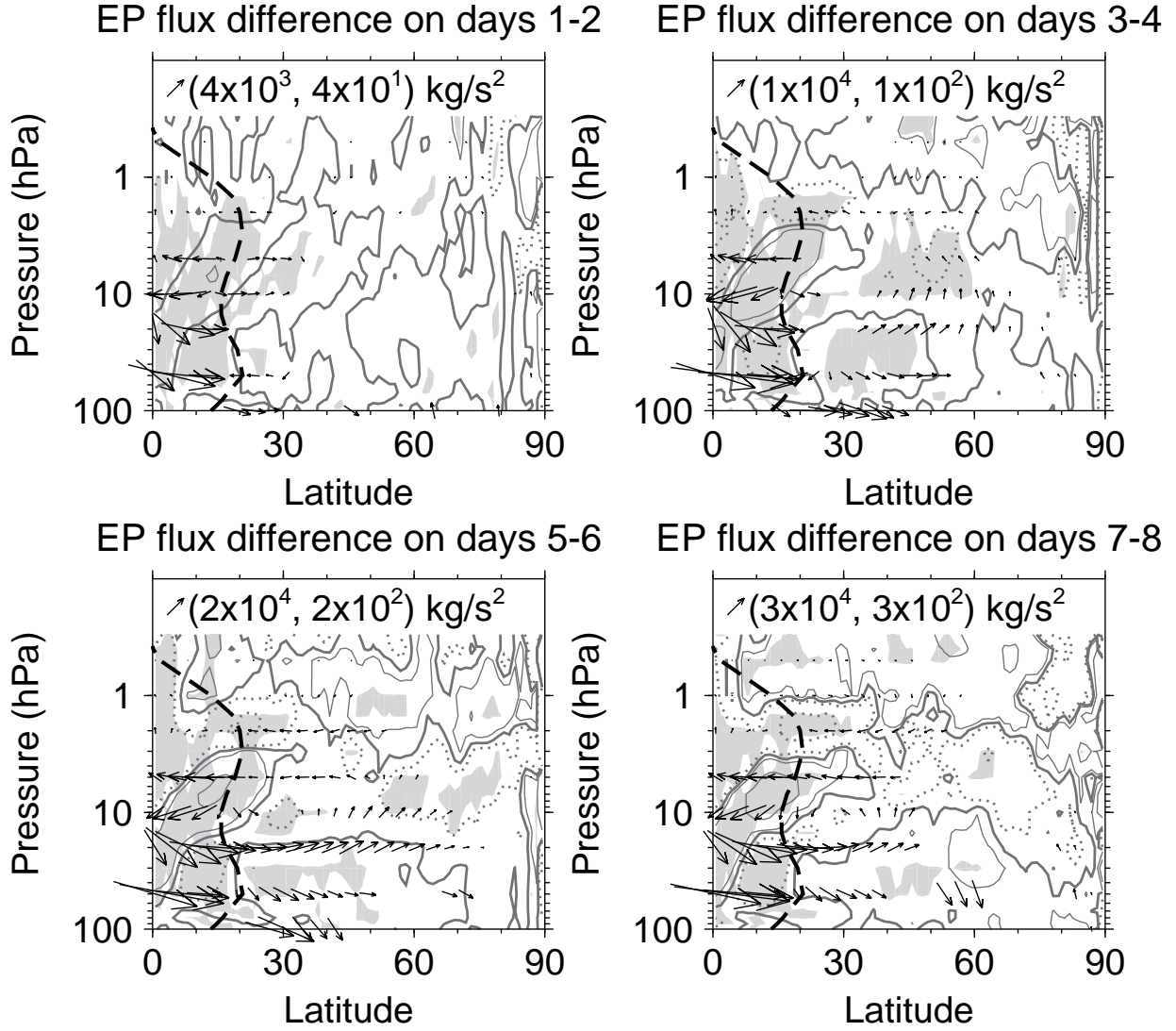


FIG. 10. Ensemble mean differences between branch runs nudged towards the QBO-E equatorial wind profile and the ClimEq run averaged over each two day interval up to 8 days following branching in EP flux (arrows, shown only where either the F^ϕ or F^z differences are statistically significant above the 95% level) and D_F (contours, at 0, ± 0.02 and ± 0.1 m/s/day, with negative contours dotted and the zero contour thickened). The thick dashed line shows the zero wind line in the days 1–8 mean ZMW in the ClimEq run. The EP flux differences are shown at pressures 0.5, 1, 2, 5, 10, 20, 40 and 100 hPa and every 3.75° in latitude. A reference arrow is shown in the top left of each plot along with its (F^ϕ, F^z) values. Shading shows where D_F differences are statistically significant at the 95% level.

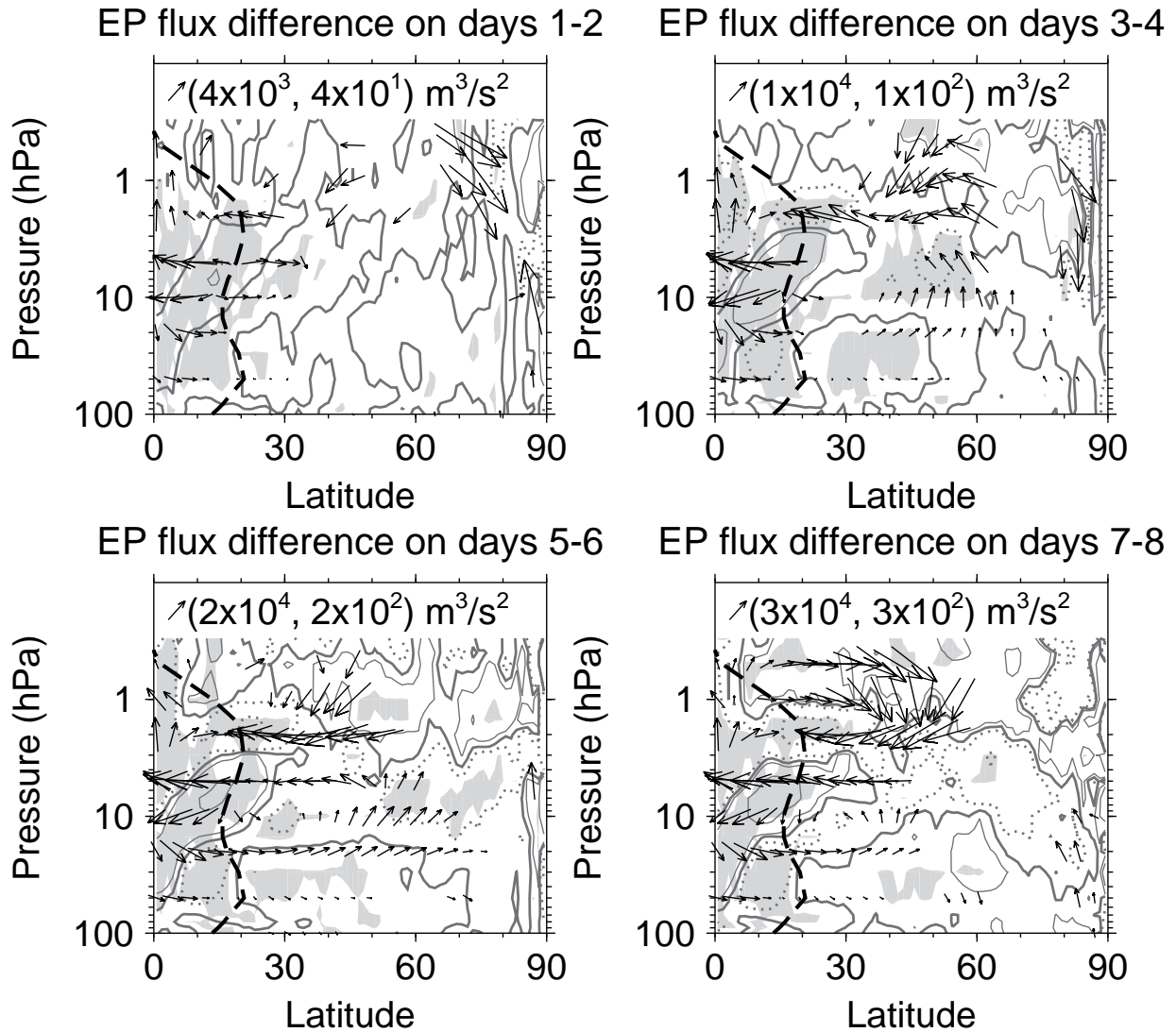


FIG. 11. As in figure 10 but using “acceleration scaling” of the EP flux vectors as defined by Gray et al. (2003), which indicates the zonal acceleration associated with the flux. A reference arrow is shown in the top left of each plot along with the (F^ϕ, F^z) values it would have at the Equator at 10 hPa.